Photoinduced Electron Transfer in Supramolecular Ruthenium-Porphyrin Assemblies.

*Diego Rota Martir,[a] Mattia Averardi,[a] Daniel Escudero,[b] Denis Jacquemin[b,c] and Eli Zysman-Colman[a]**

[a] Organic Semiconductor Centre, EaStCHEM School of Chemistry, University of St Andrews, St Andrews, Fife, KY16 9ST, UK, Fax: +44-1334 463808; Tel: +44-1334 463826; E-mail: eli.zysman-colman@st-andrews.ac.uk;
URL: http://www.zysman-colman.com
[b] CEISAM UMR CNRS 6230, Université de Nantes, 2 rue de la Houssinière, BP 92208, 44322 Nantes Cedex 3, France
[c] Institut Universitaire de France, 1, rue Descartes, 75005 Paris Cedex 5, France

Abstract. We present dynamic supramolecular systems composed of a Ru(II) complex of the form of $[Ru(dtBubpy)_2(qpy)][PF_6]_2$ (where dtBubpy is 4,4′-di-*tert*-butyl-2,2′-dipyridyl and qpy is 4,4':2',2'':4'',4'''-quaterpyridine) and zinc tetraphenylporphyrins (ZnTPP), through non-covalent interactions between the distal pyridine moieties of the qpy ligand the zinc of ZnTPP. The optoelectronic properties of the assemblies and the electronic interactions between the chromophoric units have been comprehensively characterized by computational investigations, and steady-state and time-resolved emission spectroscopy. Upon photoexcitation of ZnTPP, electron transfer to the ruthenium center is thermodynamically favorable and, as a result, strong emission quenching of both units occurs.

Introduction.

Multi-chromophoric donor-acceptor systems composed of well-defined photophysically-active units have served as surrogates to probe the nature of the photoinduced energy transfer (PET) and electron transfer (PeT) processes found in natural photosynthetic organisms. These same systems are also of great interest as dyes in solar

energy conversion applications.[1] Many of these artificial systems are formed by combining metallo-porphyrins with others photo- and redox-active species, such as Ru, Ir or Re complexes and, following this approach, a wide array of multi-component assemblies has been explored to mimic the light-harvesting exhibited by photosynthetic organisms.[2] However, in most of these cases the complexes are covalently connected along the porphyrin plane and, surprisingly, little is still known about their electronic communications upon non-covalent axial coordination to the porphyrin.[3]

We recently reported dynamic [Ir]···[ZnTPP] and [Ir]···[ZnTPP]$_2$ dyad and triad systems, Figure **1a**, composed of a cationic iridium complex of the form [Ir(dFppymes)$_2$(qpy)]PF$_6$ (where dFppymes is 2-(4,6-difluorophenyl)-4-mesitylpyridinato and qpy is 4,4':2',2'':4'',4'''-quaterpyridine) and zinc tetraphenylporphyrin, ZnTPP. [4] We showed that in these systems only self-absorption occurs between the [Ir] donor and ZnTPP acceptor.[4] PeT from [Ir] to ZnTPP is not thermodynamically favorable while PeT from ZnTPP to [Ir] was found to be exergonic (ΔG_{CS} = -0.68 V); however there was no experimental evidence to support the formation of the charge-separated [ZnTPP]$^+$-[Ir]$^-$ state. One possible explanation of this facts is that the PeT process might not be fast enough to compete with the other deactivation processes.

By contrast, when zinc tetratolylporphyrin (ZnTPP) is either covalently or non-covalently connected to a ruthenium(II) tris-bipyridyl complex (Figure **1b**), PeT from ZnTPP to the ruthenium center is experimentally observed at an ultrafast time scale (< 100 ps).[5] Many other examples of systems composed of metallo-porphyrins and ruthenium(II) polypyridine conjugates have been investigated.[6] In these systems, as a result of the formation of charge-separated state following PeT from the porphyrin units to the ruthenium moieties,

the phosphorescence of the ruthenium complexes is quenched and only weak porphyrin-centered luminescence is generally detected.

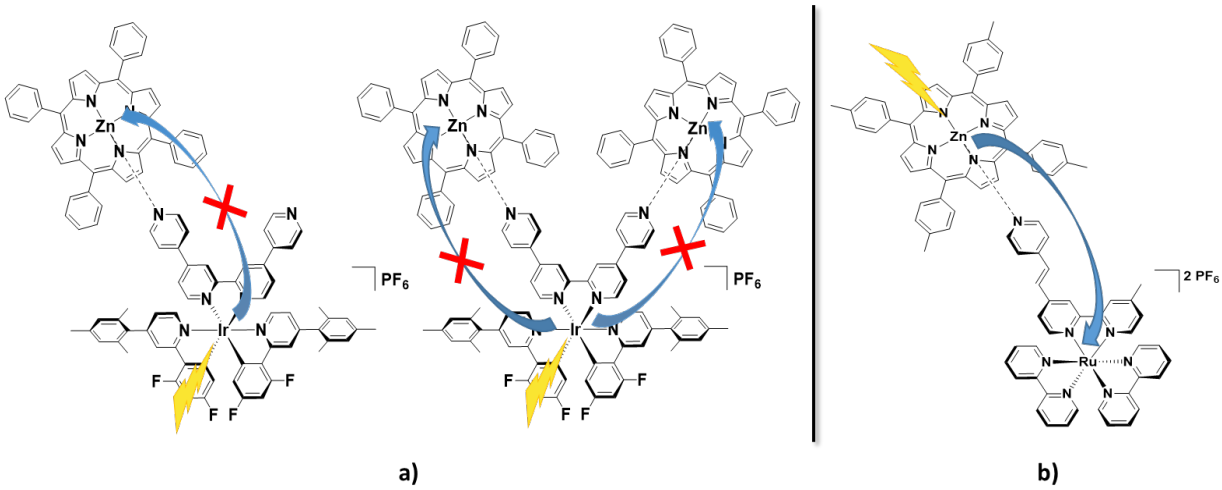

Figure **1**. **a**) Schematic representation of the absence of electron transfer in the supramolecular iridium-zinc assemblies.[4] **b)** Schematic representation of PeT observed in the ruthenium-zinc assembly.[5a]

With this in mind, we report the self-assembly and the photophysical investigation of analogous systems to those reported in Figure **1a**, based on non-covalent axial coordination between ZnTPP as the donor unit and the ruthenium complex $[Ru(dtBubpy)_2(qpy)]2PF_6$ (where dtBubpy is 4,4'-di-*tert*-butyl-2,2'-bipyridine) as the acceptor moiety (Charts **1** and **2**). These multi-chromophoric systems are of particular interest as models of supramolecular dyes used in artificial photosynthesis and photoelectrochemical devices. In particular, the subsequent replacement of the dtBubpy ligands in **1** with dcbpy (2,2'-bipyridine-4,4'-dicarboxylic acid) ligands would allow us to transfer this fundamental study of the electronic communication between the ruthenium complex and ZnTPP directly into a DSSC application.[7] This design contributes to an improved absorption profile and therefore

enhanced short circuit current by combining the absorption profiles of both ZnTPP and the ruthenium complex.[2c, 8]

We also prepared $[Ru(dtBubpy)_3][PF_6]_2$, **2**, as a negative control molecule in the form of the "non-assembly **2a**" (Chart **2b**) to verify the presence/absence of electronic communication between **1** and ZnTPP as a result of axial coordination to Zn.

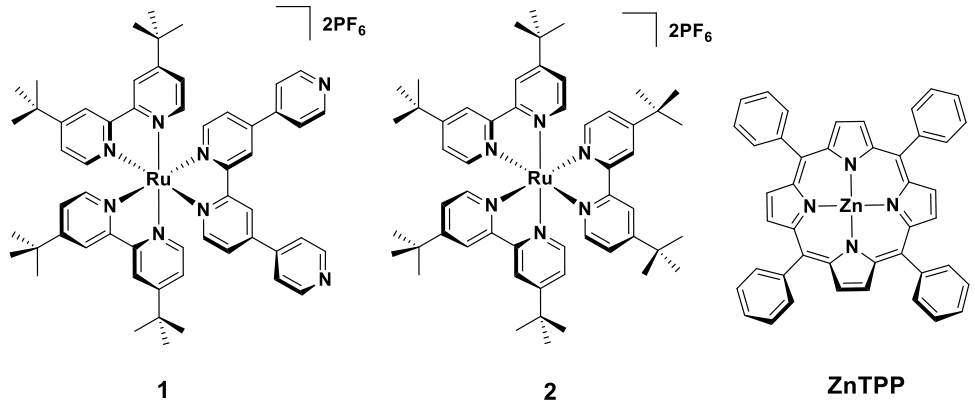

Chart **1**. Chemical structures of the reference mononuclear Ru(II) complexes **1** and **2** and ZnTPP under investigation in this work.

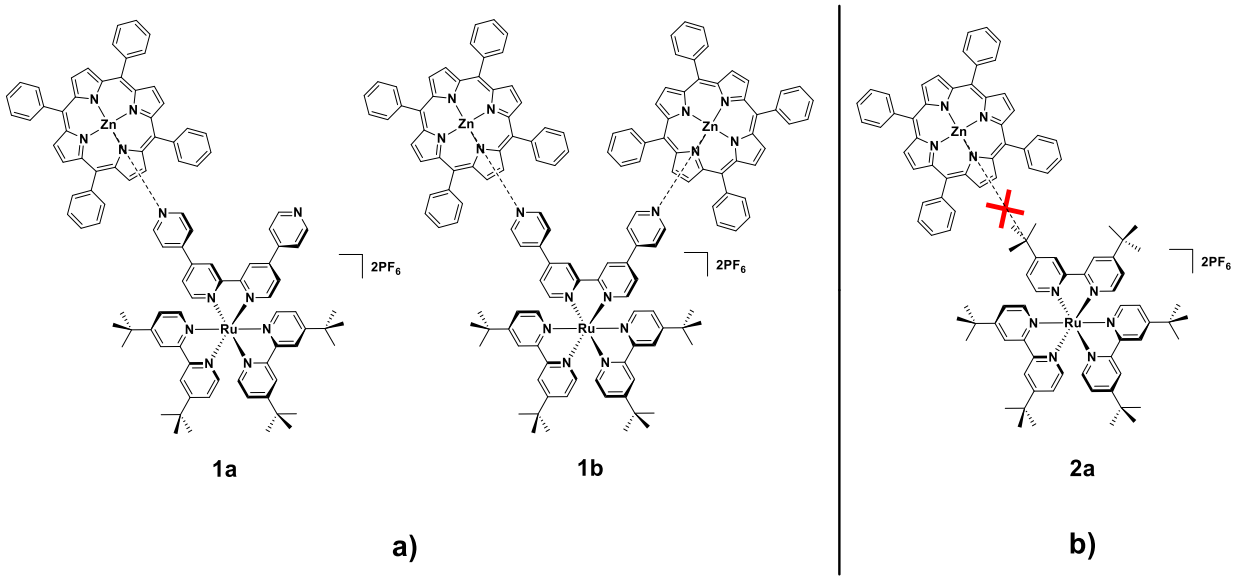

Chart **2**. **a)** Chemical structures of the assemblies **1a** [Ru(dtBubpy)$_2$(qpy)][PF$_6$]$_2$: ZnTPP 1:1 ratio and **1b** [Ru(dtBubpy)$_2$(qpy)][PF$_6$]$_2$: ZnTPP 1:2 ratio. **b)** Chemical structure of complex **2** mixed with ZnTPP (**2a**).

Results and Discussion

Self-assembly investigation by ^{1}H NMR spectroscopy.

The assemblies **1a** and **1b** were rapidly obtained after mixing **1** with one or two equivalents of ZnTPP, respectively, in CD_2Cl_2 at room temperature. The four *tert*-butyl moieties present in **1** conferred the requisite solubility in CD_2Cl_2, a solvent chosen to not interfere with the axial coordination of the distal pyridines present in **1** with ZnTPP. The formation of the assemblies was monitored by ^{1}H NMR, 2D COSY, HMBC and HMQC spectroscopies (^{1}H NMR, 2D COSY, HMBC and HMQC spectra are reported in the SI).

^{1}H NMR titration experiments of ZnTPP (from 0.1 to 2.5 equivalents, ranging from 0 to 9.44 mM) into a 3.06 mM solution of **1** in CD_2Cl_2 results in a broadening and gradual up-field shift of the proton resonances associated with **1** (Figure **2**). As expected, due to the axial coordination of the pyridine ring to ZnTPP, the proton resonances associated with the qpy moiety (H^a, H^b, H^c, H^d in Figure **2**) were shifted the most up-field. The ^{1}H NMR titration data extracted from the chemical shift of the resonance of $^1H^a$ (Figure **S13**, from δ 8.77 to δ 7.84 ppm) could be fitted to a sequential binding model (Figure **S14a**) affording equilibrium constants of 7200 ± 300 M^{-1} for the formation of **1a** from **1** and ZnTPP and 2500 ± 350 M^{-1} for the formation of **1b** from **1a** and ZnTPP. Speciation plots for the formation of **1a** and **1b** as a function of the initial concentration and stoichiometry of the mixture have been

determined (Figure **S14b,c**). For solutions containing 1:1 mixture of **1** and ZnTPP, **1a** is the dominant complex at all concentrations between 100 µM and 100 mM. For solutions containing a 1:2 mixture of **1** and ZnTPP, **1a** is the dominant complex at concentrations below 600 µM and **1b** is the dominant complex between this concentration and 100 mM.

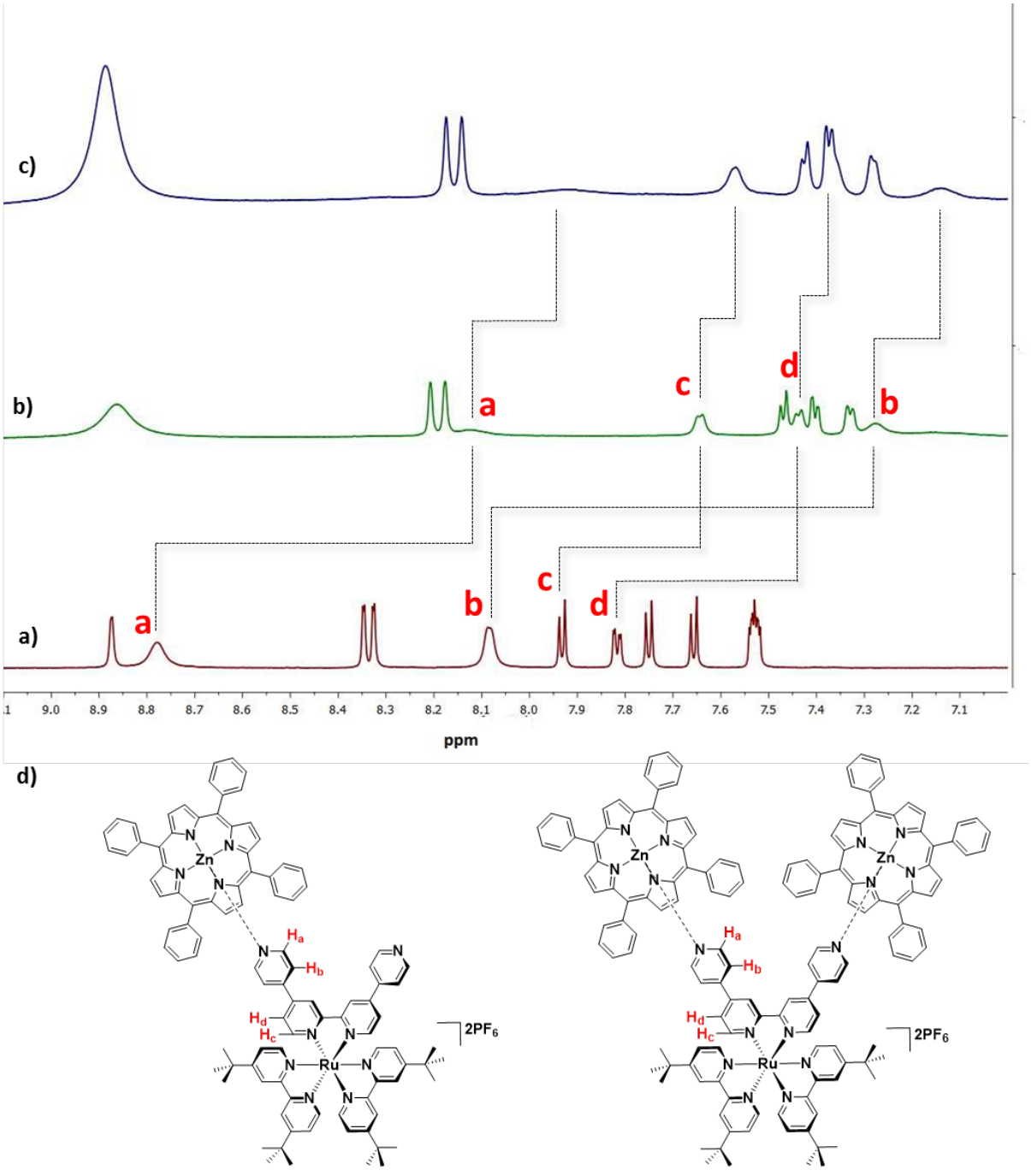

Figure **2**. ^{1}H NMR spectra in CD_2Cl_2, 500 MHz at 298 K. The concentration of **1** was kept constant at 3.06 mM. **a**) ^{1}H NMR spectrum of **1**; **b**) ^{1}H NMR spectrum of the assembly **1a**,

[ZnTPP] = 3.06 mM; **c**) ^{1}H NMR spectrum of the assembly **1b**, [ZnTPP] = 6.12 mM; **d**) chemical structures of **1a** and **1b**. The assignments correspond to the labelling shown in **d**).

As illustrated in Figure **2b**, the ^{1}H NMR spectrum for **1a** is relatively simple, indicating local C_2 symmetry around the ruthenium centre. This observation suggests that the exchange of bound and unbound ZnTPP is fast on the NMR timescale and that the ^{1}H NMR spectrum observed reflects a mixed speciation of ZnTPP – both free ZnTPP and ZnTPP bound to **1**. When **1** and ZnTPP are mixed in a 1:1 ratio at a concentration of 3.06 mM (NMR spectrum shown in Figure **2b**), a speciation of **1**:**1a**:**1b** = 0.04:1:0.1 is present, whereas when a second equivalent of ZnTPP is added (NMR spectrum shown in Figure **2c**), a speciation of **1**:**1a**:**1b** = 0.03:0.3:1 is obtained.[9] As expected, the association constants obtained for the assemblies **1a** and **1b** are very close to the values reported for the analogous assemblies illustrated in Figure **1** and similar to the values reported for the coordination between other N-donor ligands and ZnTPP, ranging from $K_a = 10^2$ to 10^5 M^{-1}.[3b] Expectedly, when **2** was mixed with two equivalents of ZnTPP no change was observed in the ^{1}H NMR spectra (Figure **S15**).

Optoelectronic properties.

Absorption.

The optoelectronic properties of ZnTPP, **1**, **1a**, **1b**, **2** and **2a** have been investigated in DCM solutions at room temperature and the results are summarized in Table **S1**. The UV-visible absorption spectra of **1** and **2** (Figure **3**) are both characterized by an intense band at *ca*. 285 nm assigned to a spin-allowed ligand-centered π–$\pi*$ transition localized on the

dtBubpy ligand and a broad band in the visible region, at *ca.* 440 nm and 494 nm for **1** and at *ca.* 432 and 469 nm for **2**. These transitions are assigned to the typical metal-to-ligand charge transfer transition (^{1}MLCT) to the dtBubpy ligand for **2** whereas, as theoretically predicted, the ^{1}MLCT bands for **1** involve both the dtBubpy and the quaterpyridine ligands.[10] Indeed, time-dependent density functional theory (TD-DFT) calculations on complex **1** corroborate the nature of the main UV-Vis bands (see Table **S3** in the ESI). The CT absorption of **1** is red-shifted (λ_{max} = 439 nm and 493 nm) compared to **2** (λ_{max} = 434 nm and 465 nm) due to the enhanced conjugation present in the qpy ligand.[10c, 11] The absorption spectra of 1:1 and 1:2 ratios of **1** and ZnTPP at 10^{-6} M where less than 1% of ZnTPP is bound to **1**, show the expected superposition of the respective absorption spectra of the two complexes (Figure **3**).

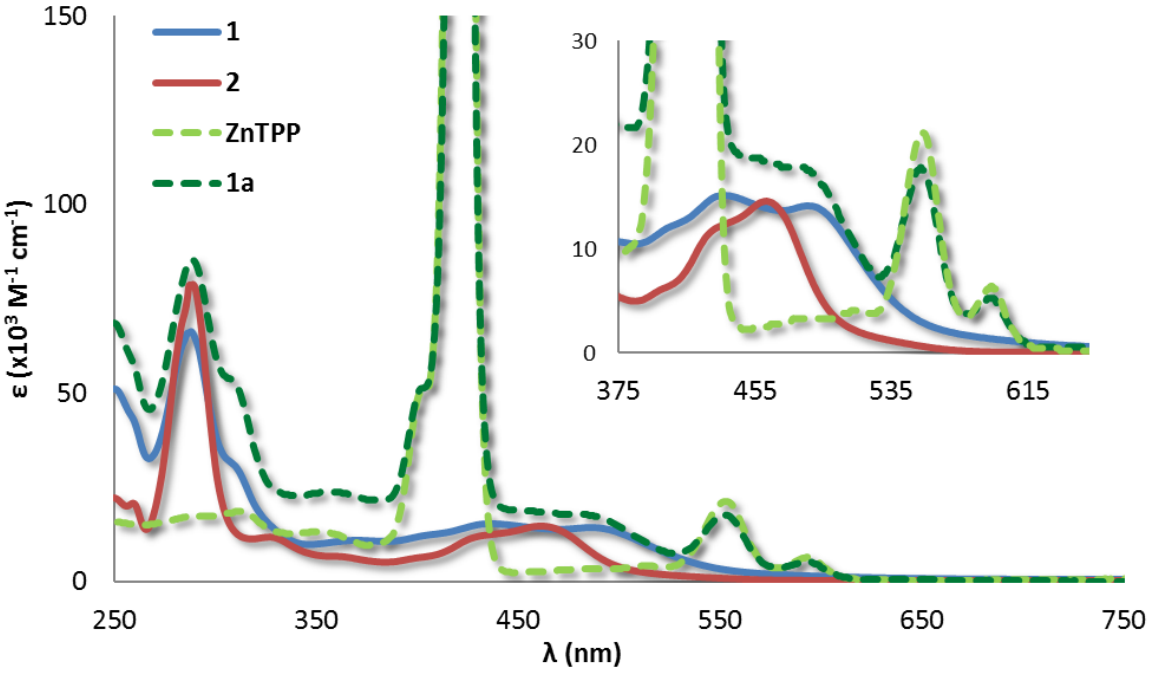

Figure **3**. UV-Vis spectra of $[Ru(dtBubpy)_2(qpy)]2PF_6$ (**1,** in solid blue line), $[Ru(dtBubpy)_3]_2PF_6$ (**2,** in solid red line), ZnTPP (dashed light-green line) and **1** : ZnTPP = 1:1 (**1a**, dashed green line) collected in CD_2Cl_2 at 298 K with a concentration on the order of 10^{-6} M.

Electrochemical properties.

The ground-state electronic communication between [Ru] and ZnTPP in **1a** and **1b** has been investigated by cyclic voltammetry (CV) and differential pulse voltammetry (DPV) in deaerated DCM solution at a concentration of 1.24 x 10^{-3} M, a concentration where ZnTPP is completely bound to **1** and where **1**, **1a** and **2a**, are present in a ratio of **1**:**1a**:**1b** = 0.02:0.1:1 when **1** and ZnTPP are mixed in a 1:1 ratio and **1**:**1a**:**1b** = 0.02:1:1.6 when a second equivalent of ZnTPP is added.[12] Similarly to the CVs of other cationic ruthenium complexes,[10b, 13] **1** and **2** exhibit a one-electron reversible oxidation wave at, respectively, $E^{ox}_{1/2}$ = 1.43 V and $E^{ox}_{1/2}$ = 1.37 V attributed to the Ru^{II}/Ru^{III} redox couple (Figure **S18**). The presence of the two addition *tert*-butyl groups in **2** detabilizes the oxidation compared to **1** while the distal pyridines on the qpy ligand inductively withdraw electron density leading to an anodic shift of the oxidation wave relative to **2**.[10c] Two quasi-reversible one-electron reduction waves at $E^{red}_{1/2}$ = -1.04 V and $E^{red}_{1/2}$ = -1.51 V localized on the quaterpyridine ligands are observed for **1**. A single one-electron reversible reduction at $E^{red}_{1/2}$ = -1.24 V localized on one of the dtBubpy ligands is observed for complex **2**. These redox processes are also observed in the DPV spectra illustrated in Figure **S18** and in Figure **S20** for complex **1** and **2**, respectively.

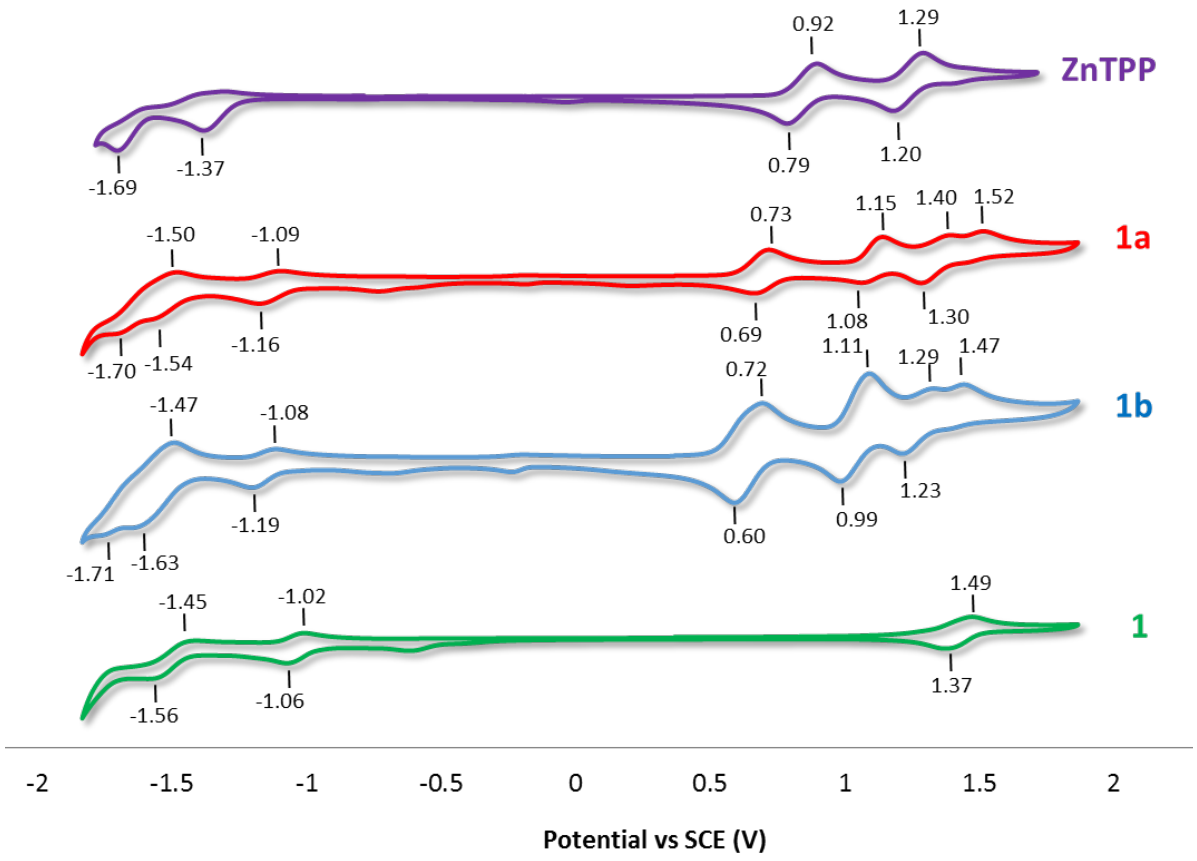

Figure **4**. CVs reported *versus* SCE for ZnTPP, **1a**, **1b** and **1** recorded at 298 K in deaerated DCM solution containing *n*-NBu_4PF_6 as the supporting electrolyte and using Fc/Fc^+ as an internal standard (Fc/Fc^+ = 0.46 V in DCM with respect to SCE).[14]

For the assemblies **1a** and **1b** the oxidation potentials localized on the ruthenium complex are slightly cathodically shifted to lower potentials compared to **1** (E^{pa} = 1.43 V for **1** *vs*. $E^{ox}_{1/2}$ = 1.35 V for **1a** and $E^{ox}_{1/2}$ = 1.26 V for **1b**, Figure **4**). However, similar to the iridium-ZnTPP assemblies that we previously studied,[4] upon ZnTPP coordination with the distal pyridine moieties of **1**,[15] the porphyrin-centered oxidation waves of both **1a** and **1b** are significantly cathodically shifted ($E^{ox}_{1/2}$ = 0.71 V for **1a**, $E^{ox}_{1/2}$ = 0.66 V for **1b** *vs*. $E^{ox}_{1/2}$ = 0.86 V for ZnTPP) while their first reduction processes are likewise cathodically shifted ($E^{red}_{1/2}$ = –1.52 V for **1a**, $E^{red}_{1/2}$ = –1.55 V for **1b** *vs*. E^{pc} = –1.37 V for ZnTPP). In addition, an extra

wave at around 1.52 V and 1.47 V can be observed respectively in the CVs of **1a** and **1b**, which are assigned to the oxidation of uncomplexed **1**. The CVs of **2** and of the "non-assembly" **2a** were also investigated in deareated DCM as a control system and, as expected, the CV **2a** contains only the superposition of the redox processes of **2** and ZnTPP, with no ground-state electronic communication between the two units (Figure **S19** and **S20**).

Prediction of photoinduced electron transfer processes.

The redox potentials and optical data were used to estimate the energetics of the electron transfer processes exhibited by the compounds under investigation.

Figure **5a** shows the lowest excited triplet-state energy of **1** and the lowest excited singlet-state energy of ZnTPP ($E_{0,0}$ energies) estimated from the intersection point between their respective absorption and luminescence spectra collected in DCM at room temperature (see below). Figure **5b** represents the inferred energies of oxidation and reduction potentials of **1** and ZnTPP obtained by CV analysis. The $E_{0,0}$ energies and the redox potentials of ZnTPP, **1**, **2** and the assemblies **1a** and **1b** are reported in Table **1**.

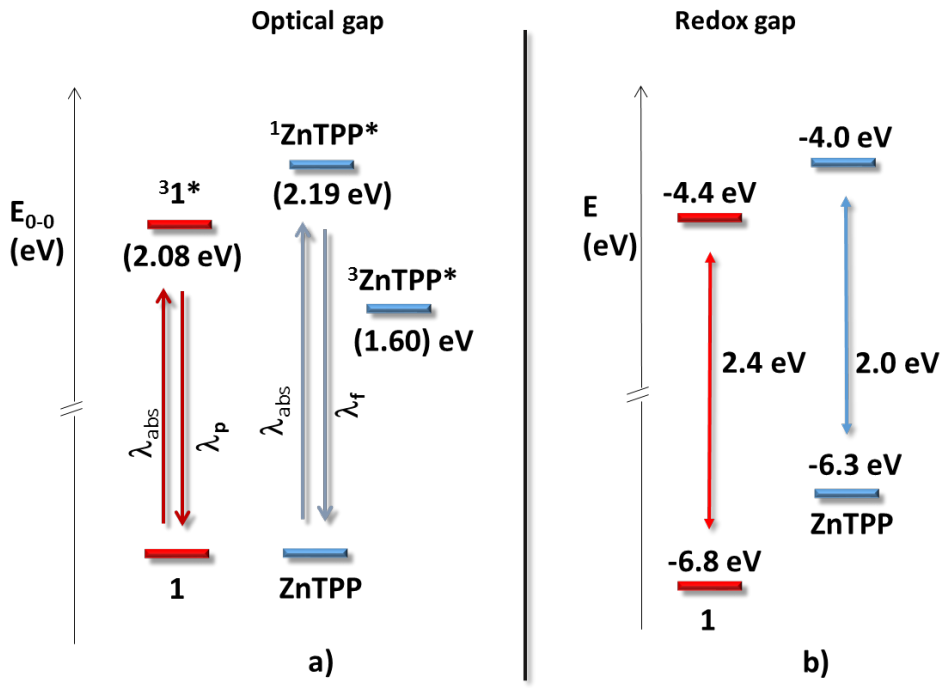

Figure **5**. **a**) Representation of the energy of the zero-zero transition ($E_{0,0}$) to the lowest excited state of complex **1** and ZnTPP obtained by spectroscopic analysis. As the energy of the lowest triplet state of ZnTPP (^{3}ZnTPP*) we used the value previously reported.[16] **b)** Representation of the energies of the first oxidation and first reduction waves, the associated redox gap and oxidation and reduction potentials of complex **1** and ZnTPP obtained by electrochemical analysis of ZnTPP and **1**. E_{HOMO} = -($E^{ox}_{pa\ vs\ Fc/Fc+}$ + 5.39) eV, E_{LUMO} = -($E^{red}_{pc\ vs\ Fc/Fc+}$ + 5.39) eV.[17]

The oxidation and reduction potentials of ZnTPP are located at -6.3 and -4.0 eV, respectively whereas for **1**, both these levels are stabilized at -6.8 and -4.4 eV. Therefore, for **1a** and **1b**, ZnTPP acts as the electron-donor unit while **1** acts as the electron-acceptor moiety.[18]

The free energy (ΔG_{CS}) associated with the formation of the charge-separated state $[ZnTPP]^+[Ru]^-$ can be easily calculated following the Rehm-Weller equation (**1**),[18a, 19]

$$\Delta G_{CS} = e\left[E_{1/2}(D^{+}/D^{*}) - E_{1/2}(A^{*}/A^{-})\right] - E_{0,0} + Gs \quad (\mathbf{1})$$

The excited state redox gap $e\left[E_{1/2}(D^{+}/D^{*}) - E_{1/2}(A^{*}/A^{-})\right]$ for **1a** and **1b** are nearly identical at, respectively, 1.69 and 1.68 eV. The ion-pair stabilization energy, Gs, for both **1a** and **1b** was inferred to be -0.14 eV and $E_{0,0}$ for the donor was determined to be 2.24 eV.[9] Consequently, following photoexcitation of **1a** and **1b**, electron transfer from ZnTPP to complex **1** is found to be exergonic in DCM (ΔG_{CS} = –0.56 eV for **1a** and **1b**). In addition, the kinetic of the process may also play an important role for the activation of the PeT.[20] By contrast, ΔG_{CS} = + 0.74 eV for the formation of the charge-separated state $[Ru]^{+}[ZnTPP]^{-}$ so is not a thermodynamically favorable process.

Table **1**. Electrochemical data and $E_{0,0}$ values.

Complex	E_{ox}[a] / V	E_{ox}[a] / V	E_{ox}[a] / V	E_{red}[a] / V	E_{red}[a] / V	E_{gap}[d] / V	$E_{0,0}$[e] / eV
ZnTPP	0.86[b]	1.25[b]	-	-1.37[c]	–1.79[c]	2.23	2.19
1	1.43[b]	-	-	–1.04[b]	–1.51[b]	2.47	2.08[e]
2	1.37[b]	-	-	–1.24[c]	-	2.61	2.29
1a	0.71[b]	1.12[b]	1.35[b]	–1.13[b]	–1.63[c]	1.84	2.20
1b	0.66[b]	1.05[b]	1.26[b]	–1.14[b]	–1.64[c]	1.80	2.20
2a	0.84[c]	1.22[b]	1.37[b]	–1.36[b]	-	2.20	2.24

[a]CV traces recorded in DCM solution with 0.1 M (n-Bu_4N)PF_6 at 298 K at 50 $mV{\cdot}s^{-1}$. Values are in V *vs.* SCE (Fc/Fc^{+} *vs.* SCE = 0.46 V).[14] [b]$E_{1/2} = (E_{pa} + E_{pc})/2$ and result from one-electron processes. [c]Irreversible oxidation and reduction peak potentials, E_{pa} reported for oxidation and E_{pc} reported for reduction. [d]Calculated from $E_{ox} - E_{red}$ where E_{ox} is the first oxidation potential and E_{red} is the first reduction potential.[e]$E_{0,0}$ determined from the intersection point of the absorption and emission spectra at 298 K in DCM.

Emission Studies.

Emission studies were carried out in DCM solution at a concentration of 3×10^{-4} M in order to verify experimentally the presence of PeT in **1a** and **1b**. At this concentration ZnTPP is completely bound to the ruthenium complex with a ratio of **1**:**1a**:**1b** = 0.01:1:0.01 when **1** is mixed with 1 equivalent of ZnTPP and with a ratio of **1**:**1a**:**1b** = 0.01:1.2:1 when a second equivalent of ZnTPP is added.[9] Upon photoexcitation of **1** and **2** into either their CT or LC absorption bands (at around 500 or 400 nm, respectively), broad and unstructured emissions from the ^{3}MLCT state at, respectively, 672 nm and 615 nm are observed (red lines in Figure **7**). Due to increased conjugation present in the qpy ligand, the emission of **1** is red-shifted compared to **2**. As reported in Table **S2**, the Φ_{PL} for **1** and **2** are similar at 7 and 9%, respectively. The character of the emissive state was confirmed by a DFT optimization of the lowest excited triplet-state (T_1, (see exemplarily the spin density distribution for **1** in Figure **6a**)). When ZnTPP is photoexcited into either the Soret or Q bands (λ_{exc} = 420 or 550 nm, respectively), a characteristic vibronic fluorescence is observed between 570 and 740 nm (blue lines in Figure **7**).[4]

Emission spectra acquired at different excitation wavelengths during the titration of one to three equivalents of ZnTPP into a 3×10^{-4} M solution of **1** to form the assemblies **1a** and **1b** are reported in Figure **S21 – S23**. Upon excitation of **1a** and **1b** into either the CT absorption band of [Ru (λ_{exc} = 500 nm)], the Q-band of ZnTPP (λ_{exc} = 550 nm) or the Soret band of ZnTPP (λ_{exc} = 420 nm), resulted in a significant reduction in the Φ_{PL} for ZnTPP ($\Phi_{PL(ZnTPP)}$ = 4%; $\Phi_{PL(ZnTPP)}$ < 1% in **1a** and **1b**, Table **S2**) while the emission of **1** was

completely quenched (Figure **7**). The efficient quenching of the phosphorescence of **1** and the fluorescence of ZnTPP are due to the formation of the non-emissive charge-separated state $[ZnTPP]^{+}[Ru]^{-}$ as was predicted following the Rehm-Weller equation and in agreement with the PeT processes reported for similar systems.[5, 21] Indeed, by contrast to **1**, the optimization of its lowest triplet excited state leads to a CT state (see exemplarily for **1a** in Figure **6b**). The enhanced non-radiative decay from this dark-state (that eventually leads to the formation of the charge-separated states) is responsible of the emission quenching observed in the assemblies.[22]

As a result of the strong emission quenching observed for **1a** and **1b**, no emission lifetimes could be discerned.

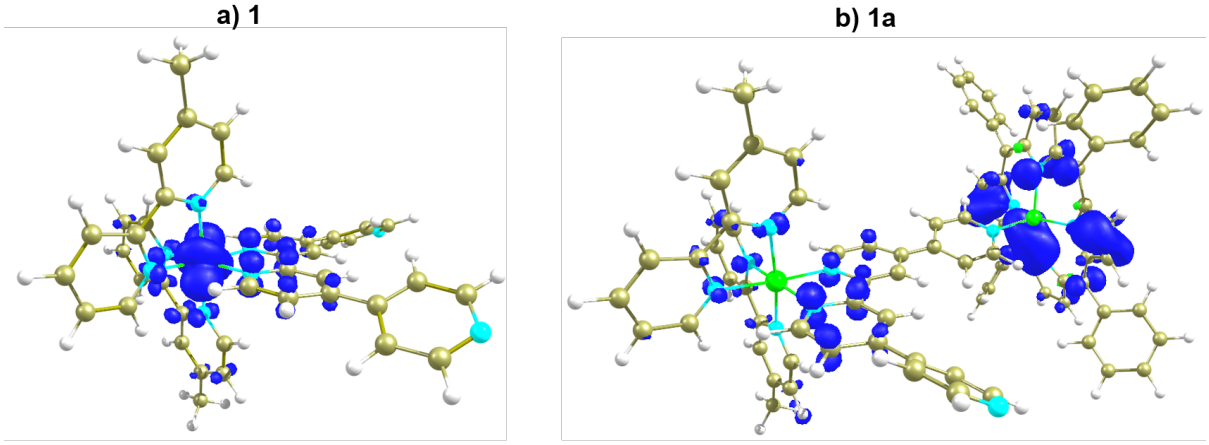

Figure **6**. Spin-density distributions [B3LYP/6-31G(d) – ecp-28-mwb for Ru] at the optimized geometry of the lowest triplet excited state of **1** (**a**) and **1a** (**b**).

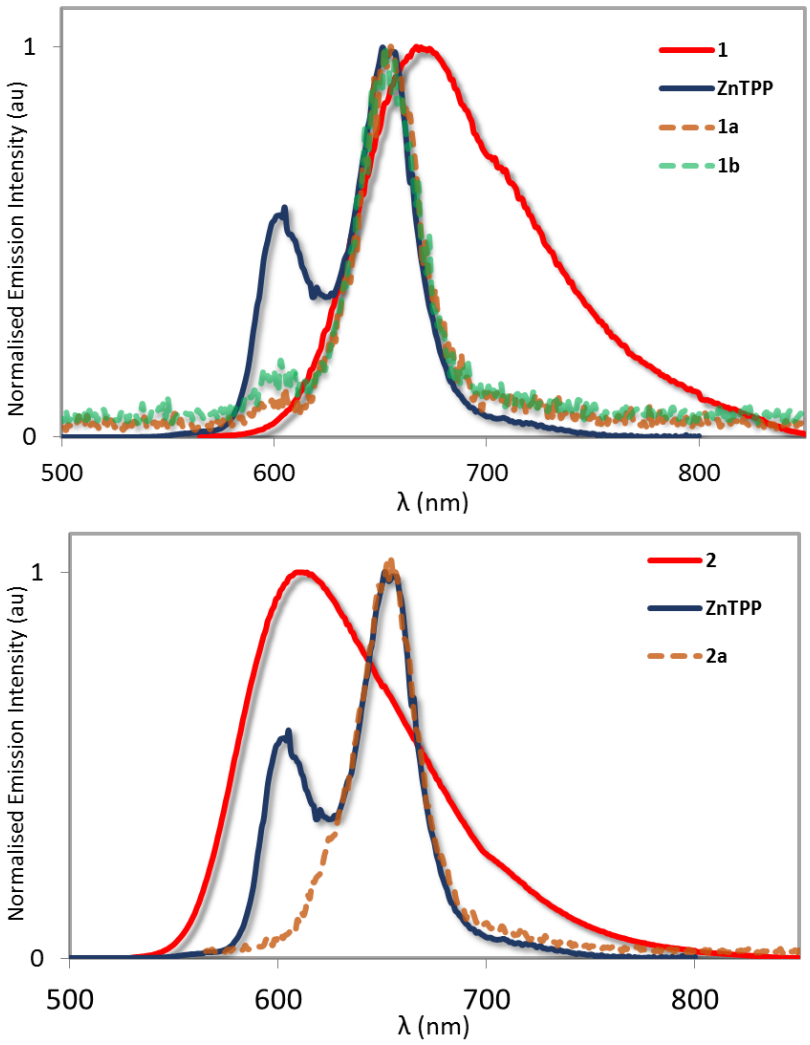

Figure **7**. a) Normalized luminescence spectra of **1** (solid red line), ZnTPP (solid blue line), **1a** (dotted orange line) and **1b** (dotted green line) recorded in degassed DCM at 298 K (λ_{ex} = 555 nm) with a concentration in the order of 3 x 10^{-4} M. b) Normalized luminescence spectra of **2** (solid red line), ZnTPP (solid blue line) and of the "non-assembly" **2a** (dotted orange line) recorded in degassed DCM at 298 K (λ_{ex} = 555 nm) with a concentration in the order of 10^{-4} M.

To discern whether the formation of the non-emissive charge-separated state observed for **1a** and **1b** is favored through the coordination of ZnTPP to the qpy, emission spectra were also collected after addition of ZnTPP to the control complex **2** (at a

concentration of 3 × 10^{-4} M) where coordination is not possible (the emission spectra are reported in Figure **S24** – **S26**). We noted that upon excitation at 420, 500 or 550 nm, the emission of **2** was likewise strongly quenched and presented similar behavior to that observed for **1a** and **1b** (Figure **7b**). Thus, we attribute the strong emission quenching of both the ruthenium complex and ZnTPP as the result of long-distance collisional processes between the two chromophoric units.[23]

Conclusions.

In conclusion, we report the synthesis and optoelectronic study of [Ru]···[ZnTPP] dyad and [Ru]···$[ZnTPP]_2$ triad supramolecular assemblies where the ZnTPP is bound to [Ru] through axial coordination of zinc metal to the distal pyridine moieties of the qpy of $[Ru(dtBubpy)_2(qpy)][PF_6]_2$. For the assemblies **1a** and **1b**, favorable PeT from ZnTPP to [Ru] is predicted (ΔG_{CS} = –0.51 eV) and evidence of emission quenching through the formation of the non-emissive charge-separated $[ZnTPP]^+[Ru]^-$ state was observed. The emission of **2** and ZnTPP were likewise quenched upon mixing at a concentration of 3 × 10^{-4} M. Thus, we can confirm that self-assembly of [Ru] and ZnTPP is not necessary to promote PeT from ZnTPP to [Ru] under our experimental conditions.

Acknowledgements

EZ-C acknowledges the University of St Andrews and EPSRC (EP/M02105X/1) for financial support. We thank the EPSRC UK National Mass Spectrometry Facility at Swansea University for analytical services. We thank Umicore AG for the gift of materials. DE thanks funding from the European Union's Horizon 2020 research and innovation programme under the Marie Sklodowska-Curie grant agreement No

700961. DJ acknowledges the European Research Council (grant: 278845) and the RFI Lumomat for financial support. This research used resources of (1) the GENCI-CINES/IDRIS, (2) Centre de Calcul Intensif des Pays de Loire (CCIPL), and (3) a local Troy cluster.

Supporting Information. Experimental section, characterisation of precursors, ligands, ruthenium complexes and supramolecular assemblies; solution NMR investigations of the assemblies; determination of the association constants; absorption and emission studies at different concentrations, emission studies and electrochemical characterization; computational details.

References.

(1). (a) L. Flamigni, J.-P. Collin and J.-P. Sauvage, *Acc. Chem. Res.*, 2008, **41**, 857-871; (b) F. Nastasi, F. Puntoriero, S. Campagna, S. Schergna, M. Maggini, F. Cardinali, B. Delavaux-Nicot and J.-F. Nierengarten, *Chem. Commun.*, 2007, 3556; (c) Y. Kuramochi, A. S. Sandanayaka, A. Satake, Y. Araki, K. Ogawa, O. Ito and Y. Kobuke, *Chemistry*, 2009, **15**, 2317-2327; (d) J. Otsuki, T. Akasaka and K. Araki, *Coord. Chem. Rev.*, 2008, **252**, 32-56; (e) P. K. Poddutoori, L. P. Bregles, G. N. Lim, P. Boland, R. G. Kerr and F. D'Souza, *Inorg. Chem.*, 2015, **54**, 8482-8494.
(2). (a) J. Henderson and C. P. Kubiak, *Inorg Chem*, 2014, **53**, 11298-11306; (b) E. Iengo, E. Zangrando, M. Bellini, E. Alessio, A. Prodi, C. Chiorboli and F. Scandola, *Inorg. Chem.*, 2005, **44**, 9752-9762; (c) A. F. Nogueira, L. F. O. Furtado, A. L. B. Formiga, M. Nakamura, K. Araki and H. E. Toma, *Inorg. Chem.*, 2004, **43**, 396-398; (d) L. Flamigni, G. Marconi, I. M. Dixon, J.-P. Collin and J.-P. Sauvage, *J. Phys. Chem. B*, 2002, **106**, 6663-6671; (e) K. Chichak and N. R. Branda, *Chem. Commun.*, 2000, 1211-1212.
(3). (a) S. A. Rousseaux, J. Q. Gong, R. Haver, B. Odell, T. D. Claridge, L. M. Herz and H. L. Anderson, *J Am Chem Soc*, 2015, **137**, 12713-12718; (b) A. Satake and Y. Kobuke, *Tetrahedron*, 2005, **61**, 13-41.
(4). D. Rota Martir, G. J. Hedley, D. B. Cordes, A. M. Z. Slawin, D. Escudero, D. Jacquemin, T. Kosikova, D. Philp, D. M. Dawson, S. E. Ashbrook, I. D. W. Samuel and E. Zysman-Colman, *Dalton Trans.*, 2016, **45**, 17195-17205.

(5). (a) D. Kim and E.-J. Shin, *Bull. Korean Chem. Soc.*, 2003, **24**, 1490-1494; (b) D. LeGourriérec, M. Andersson, J. Davidsson, E. Mukhtar, L. Sun and L. Hammarström, *J. Phys. Chem. A*, 1999, **103**, 557-559.
(6). (a) J.-P. Collin, A. Harriman, V. Heitz, F. Odobel and J.-P. Sauvage, *J. Am. Chem. Soc.*, 1994, **116**, 5679-5690; (b) A. Harriman, F. Odobel and J.-P. Sauvage, *J. Am. Chem. Soc.*, 1995, **117**, 9461-9472; (c) L. Flamigni, N. Armaroli, F. Barigelletti, V. Balzani, J.-P. Collin, J.-O. Dalbavie, V. Heitz and J.-P. Sauvage, *J. Phys. Chem. B*, 1997, **101**, 5936-5943; (d) K. Araki and H. E. Toma, *J. Photochem. Photobiol., A*, 1994, **83**, 245-250; (e) T. Ben Hadda and H. Le Bozec, *Inorg. Chim. Acta*, 1993, **204**, 103-107.
(7). (a) K. Araki and H. E. Toma, *J. Coord. Chem.*, 1993, **30**, 9-17; (b) T. J. Meyer, *Acc. Chem. Res.*, 1989, **22**, 163-170.
(8). Y. Qin and Q. Peng, *International Journal of Photoenergy*, 2012, **2012**, 21.
(9). At a concentration of 3.0×10^{-4} M, **[1a]** = 1.8×10^{-4} M, **[1b]** = 1.5×10^{-4} M.
(10). (a) M. J. Lundqvist, E. Galoppini, G. J. Meyer and P. Persson, *J. Phys. Chem. A*, 2007, **111**, 1487-1497; (b) R. E. Piau, T. Guillon, E. Lebon, N. Perrot, F. Alary, M. Boggio-Pasqua, J.-L. Heully, A. Juris, P. Sutra and A. Igau, *New J. Chem.*, 2012, **36**, 2484; (c) B. J. Coe, E. C. Harper, M. Helliwell and Y. T. Ta, *Polyhedron*, 2011, **30**, 1830-1841.
(11). E. Rousset, D. Chartrand, I. Ciofini, V. Marvaud and G. S. Hanan, *Chem. Commun.*, 2015, **51**, 9261-9264.
(12). The speciation values have been obtained by plotting the concentration of the assemblies **1a** and **1b** against the concentration of the initial substrate **1** taking into account the values of the association constants $Ka' = 7.2 \times 10^{3}$ M^{-1} and $Ka'' = 2.5 \times 10^{3}$ M^{-1}. The simulations have been fitted by Gepasi software. See: P. Mendes, *Computer applications in the biosciences : CABIOS*, 1993, **9**, 563-571. At a concentration of 1.24×10^{-3} M, **[1a]** = 4.2×10^{-4} M, **[1b]** = 6.8×10^{-4} M.
(13). (a) V. Leigh, W. Ghattas, R. Lalrempuia, H. Muller-Bunz, M. T. Pryce and M. Albrecht, *Inorg Chem*, 2013, **52**, 5395-5402; (b) M. Schwalbe, B. Schäfer, H. Görls, S. Rau, S. Tschierlei, M. Schmitt, J. Popp, G. Vaughan, W. Henry and J. G. Vos, *Eur. J. Inorg. Chem.*, 2008, **2008**, 3310-3319.
(14). N. G. Connelly and W. E. Geiger, *Chem. Rev.*, 1996, **96**, 877-910.
(15). (a) F. D'Souza, S. Gadde, M. E. Zandler, M. Itou, Y. Araki and O. Ito, *Chem. Commun.*, 2004, 2276-2277; (b) C.-W. Huang, K. Yuan Chiu and S.-H. Cheng, *Dalton Trans.*, 2005, 2417-2422.
(16). V. A. Walters, J. C. de Paula, B. Jackson, C. Nutaitis, K. Hall, J. Lind, K. Cardozo, K. Chandran, D. Raible and C. M. Phillips, *J. Phys. Chem.*, 1995, **99**, 1166-1171.
(17). C. M. Cardona, W. Li, A. E. Kaifer, D. Stockdale and G. C. Bazan, *Adv. Mater.*, 2011, **23**, 2367-2371.
(18). (a) G. J. Kavarnos and N. J. Turro, *Chem. Rev.*, 1986, **86**, 401-449; (b) V. Balzani, F. Bolletta, F. Scandola and R. Ballardini, *Pure Appl. Chem.*, 1979, **51**, 299-311.
(19). S. Doose, H. Neuweiler and M. Sauer, *Chemphyschem*, 2009, **10**, 1389-1398.
(20). (a) T. X. Nguyen, S. Landgraf and G. Grampp, *Journal of Photochemistry and Photobiology B: Biology*, 2017, **166**, 28-34; (b) B. Durham, L. P. Pan, J. E. Long and F. Millett, *Biochemistry*, 1989, **28**, 8659-8665.
(21). X. Liu, J. Liu, K. Jin, X. Yang, Q. Peng and L. Sun, *Tetrahedron*, 2005, **61**, 5655-5662.
(22). D. Escudero, *Acc. Chem. Res.*, 2016, **49**, 1816-1824.
(23). G. McLendon, *Acc. Chem. Res.*, 1988, **21**, 160-167.

TOC Graphic